Journal of Chromatography, 178 (1979) 41–61

CHROM. 12,056

END-EFFECTS AND BAND SPREADING IN LIQUID COLUMN CHROMATOGRAPHY

B. COQ, G. CRETIER and J. L. ROCCA

Laboratoire de Chimie Analytique III, Equipe de Recherche Associée au C.N.R.S. (E.R.A. 474), Professeur M. Porthault, Université Lyon I, 43 Boulevard du 11 Novembre 1918, 69621 Villeurbanne (France)

and

R. KASTNER

Laboratoire de Mécanique des Sols, Département de Génie Civil et Urbanisme de l'Institut National des Sciences Appliquées, 20 Avenue Albert Einstein, 69621 Villeurbanne (France)

(Received May 22nd, 1979)

SUMMARY

The band spreading process due to velocity inequalities in column extremities where an uneven flow profile settles is described by the field shape, column diameter and mobile phase velocity. An analogue simulation with a resisting network is presented; this method makes it possible to determine the flow pattern at each column extremity. A knowledge of the flow field allows one to calculate the characteristic variance of peak broadening with a parameter λ expressing the shape of the flow field, *i.e.*, the relative magnitude of velocity inequalities. This variance is proportional to the square of the column diameter and the square of the ratio of the connecting tube and column diameters; it further depends on the permeability and thickness of porous frits in the column ends; finally, this variance depends on the mobile phase velocity; if the mobile phase velocity is low, molecular diffusion corrects the band spreading due to flow inequalities.

The peak broadening resulting from end-effects can be so important that under extreme conditions the column efficiency can be reduced more than ten-fold.

INTRODUCTION

Band spreading in chromatography originates from three phenomena: (i) molecular diffusion in the mobile phase; (ii) convective dispersion in the mobile phase due to velocity inequalities resulting from the complex flow field set up through the porous medium; (iii) a finite rate of equilibrium between the solute and the stationary phase. Under practical conditions of analysis, the relative contribution of these three factors to band spreading has been changing in recent years as the particle size of the packings used has been decreased. With large particles the mass transfer term in the stationary phase is generally the main factor in band spreading,

whereas with microparticles convective dispersion in the mobile phase is usually the most important term, so that it is now necessary to control the latter in order to limit band spreading. Whereas molecular diffusion is well defined, solute dispersion in the mobile phase has been studied by several workers who have placed different interpretations on it. The starting point of these theories was the convective band spreading that occurs in the mobile phase, at the steady state, resulting from flow velocity inequalities. This phenomenon was explained by means of classical eddy diffusion theory[1]; this explanation was refuted by Giddings[2], Knox[3] and Huber[4], whose coupling theories were the result of a thorough analysis of the inter-relation between flow and diffusion in packed beds. More recently, Horváth and Lin[5] proposed a relatively simple theory that was a modification of the classical eddy diffusion concept, assuming that a stagnant fluid space sets up in the interstices of the column packing.

For any chosen model, band spreading takes place at several levels, from the microscopic, trans-channel effects up to the macroscopic, trans-column effects between the axis and the column walls. This work deals with some aspects of dispersion by trans-column effects, some cases of which have previously been studied such as the so-called "wall-effect" by Knox and Parcher[6], and also the bending or coiling of columns, particularly for preparative-scale gas chromatography, as described by Giddings[7]. The tendency to use columns with a low aspect ratio as in analytical and preparative-scale liquid chromatography confers greater importance on these so-called "end-effects" than they had previously; this last phenomenon was previously pointed out by some workers in studies of liquid column chromatography[8–11] and flow field fractionation[12]. The aims of this work were to give a theoretical interpretation to band spreading phenomena at both column extremities, to show that these are related to the particular shape of the flow field in this part of the column, and to emphasize the influence of porous frits on the flow profile and consequently on band spreading.

FLOW FIELD AND BAND SPREADING

Generally, when band spreading is connected with the flow field, the latter is assumed to be regular at the macroscopic level, *i.e.*, the mean velocity vector is parallel at each point of the same cross-section with the column axis. This simplifying hypothesis is justified in most instances but it is not suitable at the two column extremities and could result in critical errors in the interpretation of band broadening with columns of low aspect ratio; in these two zones, an uneven flow pattern sets up, which involves a particular contribution to peak variance and then to the total height equivalent to a theoretical plate (HETP).

Band spreading process

Other studies of flow through porous media[13] suggest that an unequal flow profile sets up in column extremities (Fig. 1) and the eluted band undergoes hydrodynamic deformation. In this assumption the sample is radially dispersed; sample stream B approaching the column wall travels through a longer path than sample stream A moving through the centre of the column. Hence the solute molecules travelling in stream B are late and the eluted band undergoes a deformation (Fig. 1). This spreading model based on path inequalities of streamlines assumes that flow is

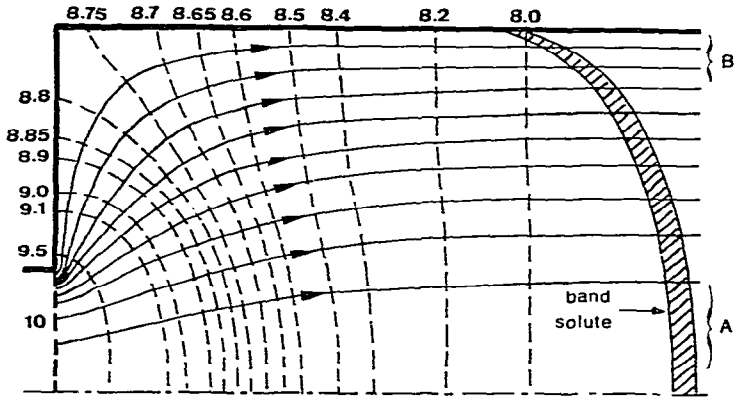

Fig. 1. Flow net of equipotential curves and streamlines in the column top; section change ratio $\beta = 0.33$.

laminar, *i.e.*, there is no fast mass transfer between streamlines, and that the radial transport of molecules depends only on molecular diffusion and possibly on eddy diffusion. This process seems to be supported by the experimental results; Fig. 2 shows the shape of the eluted band in a 4 cm I.D. column fed by means of a 2 mm I.D. connection tube; under these conditions, end-effects contribute considerably to the eluted band distortion. The tailing band profile is detrimental to the separating power of the overall chromatographic system.

Coupling and band spreading

The column efficiency is commonly expressed by means of HETP, which is related to the variance, σ^2, of band spreading by

$$H = \frac{\sigma^2}{L} \tag{1}$$

where L is the column length. The particular contribution H_E to the overall plate height caused by non-uniform flow and anastomosis in packed bed is given by:

$$H_E = \frac{2\lambda d_p}{1 + \omega \left(\frac{D_m}{u d_p}\right)^n} \tag{2}$$

where λ is a measure of the flow inequality in the bed, ω a structural parameter of the packing, d_p the mean particle diameter, D_m the molecular diffusivity of the solute in the eluent and n a value expressing the coupling in the mobile phase between velocity inequalities, molecular diffusion and the flow mechanism in the packed bed; $n = 0.33$ according to Horváth and Lin[5] and Knox[3], 0.5 according to Huber[4] and 1 according to Giddings[2]; as no theoretical interpretation appears indisputable, empirical measurements of n seem as valid as theoretical demonstrations.

The peak variance, σ^2, is more suitable than plate height for describing band spreading resulting from end-effects because this particular variance does not depend

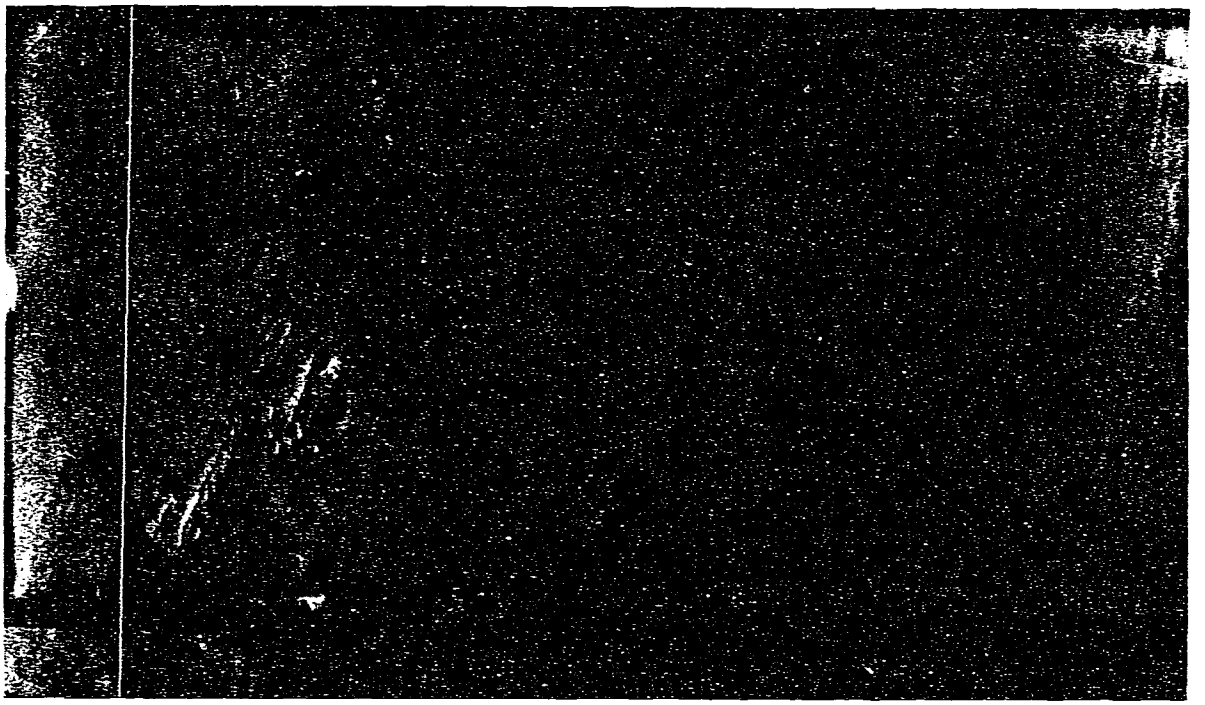

Fig. 2. Shape of the chromatographic band of an unretained solute in a 4 cm I.D. column fed by means of a 2 mm I.D. connection tube. Stationary phase, LiChroprep, 15–25 μm; mobile phase, ethyl acetate; sample, 200 μl of Sudan Red dissolved in the mobile phase; flow-rate, 12.5 ml/min. Apparatus, Jobin Yvon Chromatospac Prep 10 with a laboratory-modified column head.

on column length. For any convective mixing in the mobile phase the expression of peak variance is

$$\sigma^2 = \frac{2\lambda d_p L}{1 + \omega \left(\frac{D_m}{u d_p}\right)^n} \tag{3}$$

In order to examine the validity of this variance expression with the particular nature of the flow field in the column extremities, it is necessary to make some modifications.

(i) λd_p expresses the fact that at the steady-state velocity inequalities exist in a moving fluid with a relative magnitude λ and depend on the particle diameter; the particular shape of the flow field in the column extremities does not depend on particle size (to a great extent) and is affected only by a change in the cross-section of the tubing or column, so it is necessary in eqn. 3 to replace the term λd_p with $\lambda_1 d_c$, where λ_1 depends only on the ratio, β, between connecting tube diameter and the column diameter ($\beta = d_a/d_c$).

(ii) σ^2 is proportional to L when the spreading process takes place uniformly all along the column; however, the band spreading due to end-effects is located only in a limited area which is proportional to the column diameter, so in eqn. 3 we must replace the length L with $\lambda_2 d_c$; λ_2 depends on β in the same way as λ_1.

Let $\lambda_1\lambda_2 = \lambda$, then the correct expression for the peak variance, $\sigma^2_{e.c.}$, characteristic of end-effects is given by

$$\sigma^2_{e.c.} = \frac{2\lambda d_c^2}{1 + \omega\left(\frac{D_m}{ud_p}\right)^n} \tag{4}$$

and it is possible to determine theoretically λ, which depends only on the flow field shape and consequently on β.

VELOCITY INEQUALITIES AND FLOW FIELD

The parameter λ accounts for the relative magnitude of velocity inequalities at the macroscopic level and depends only on the flow profile in the column extremities; hence the calculation of λ implies a knowledge of the macroscopic flow field.

Determination of flow field

The flow field is totally defined when the direction and modulus of velocity vector are known at each point of the porous medium; this determination requires the resolution of the Navier-Stokes equation. This is too complex and it is better to make rough estimates of the various flow differences: generally simplified models are used, allowing either a partial description of the overall phenomenon or a precise determination of some particular effects. For example, it is possible to determine accurately the trans-column effect, which is a manifestation of column-wide flow differences; this has already been done for the wall-effect and for the bending or coiling of chromatographic columns. We can determine likewise the flow pattern in column extremities.

The chromatographic flow is nearly always laminar in most practical instances; a knowledge of laminar flow at the macroscopic level in a homogeneous and isotropic porous medium involves solving the following differential equation in cylindrical coordinates:

$$\frac{\partial^2 \varnothing}{\partial r^2} + \frac{1}{r} \cdot \frac{\partial \varnothing}{\partial r} + \frac{\partial^2 \varnothing}{\partial z^2} = 0 \tag{5}$$

where $\varnothing$ represents the hydraulic potential. The boundary conditions for solving eqn. 5 are as follows: (i) the packed bed is contained within an impermeable boundary at $r = r_c$, where r_c is the column radius; and (ii) in both column extremities, collecting and feeding sections are equipotential surfaces.

The analytical resolution of the differential eqn. 5 obtained by means of various mathematical methods allows one to obtain an exact solution of the problem. However, such a result is obtained only in some easy cases, and in most cases it is necessary to use approximate methods of resolution:

(i) The analogue method consists in replacing the flow study by a study of a similar physical phenomenon; this phenomenon must be represented by the same equation, must be easy to simulate and must be more accessible for measurements. The most common method is the electrical analogy: in a conducting homogeneous

and isotropic medium, the field of electrical potential, U, satisfies the following equation (in cylindrical coordinates):

$$\frac{\partial^2 U}{\partial r^2} + \frac{1}{r} \cdot \frac{\partial U}{\partial r} + \frac{\partial^2 U}{\partial z^2} = 0 \tag{6}$$

which is identical with eqn. 5. The flow study can be replaced with a study of an electrical potential field.

(ii) The numerical method allows the determination of hydraulic potential at each point. The continuous medium is replaced by juxtaposition of elements in which the potential answers a simple law. Eqn. 5 is written in each element and so a linear system with n equations and n unknowns (parameters defining the potential in each elementary domain) is obtained. The analytical integration of eqn. 5 is replaced with the always possible resolution of a linear system.

(iii) The mixed method of resisting network is a combination of the two previous ones: the equation set obtained by finite difference approximation is solved by means of an analogue computer: a resisting network. We have chosen this last method. Two steps must be considered: (a) passing to finite differences; this allows one to state the flow problem in a numerical form; and (b) the resolution of this numerical problem by a resisting network.

Huard de la Marre[14] showed that the flow law in point 0 of a porous medium is similar to the Kirchoff law applied in node 0 of a resisting network; this assumes a judicious choice of resistance values and continuity of the hydraulic potential function, $\varnothing$.

Huard de la Marre[14] and Liebmann[15] gave rules for calculating resistance values necessary for the study of two- and three-dimensional flow. After coordinates changes:

$$\left.\begin{aligned} Z &= z \\ \xi &= \log r \end{aligned}\right\} \tag{7}$$

eqn. 5 is written as

$$\frac{1}{r^2} \cdot \frac{\partial^2 \varnothing}{\partial \xi^2} + \frac{\partial^2 \varnothing}{\partial z^2} = 0 \tag{8}$$

Hence the hydraulic potential study is replaced with an electrical potential study in an even resisting network (Fig. 3). The resistance values were given by Liebmann[15] in the following form:

$$\left.\begin{aligned} R_1 &= \frac{\log (r_1/r_0)}{Z_1 - Z_4} \cdot R; \qquad R_2 = \frac{4(Z_2 - Z_0)}{(r_1 - r_3)(2r_0 + r_3 + r_1)} \cdot R; \\ R_3 &= \frac{\log (r_0/r_3)}{Z_1 - Z_4} \cdot R; \qquad R_4 = \frac{4(Z_0 - Z_4)}{(r_1 - r_3)(2r_0 + r_3 + r_1)} \cdot R \end{aligned}\right\} \tag{9}$$

where R is a resistance value called the network constant. These equations are not valid on the $0Z$ axis, where Liebmann replaced them with

$$\left.\begin{aligned} R_1 &= \frac{2R}{Z_1 - Z_4}; \qquad R_2 = \frac{4(Z_2 - Z_0)\,R}{r_1^2}; \\ R_4 &= \frac{4(Z_0 - Z_4)\,R}{r_1^2} \end{aligned}\right\} \tag{10}$$

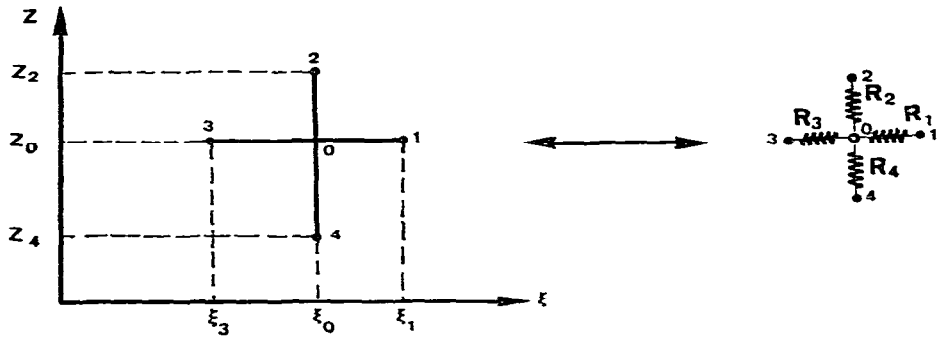

Fig. 3. Analogy between an element of porous medium and a node of resisting network.

In the particular case of even and axisymmetrical flow, there is a current function $\psi(r, z)$ which is harmonic like the potential function:

$$\frac{\partial^2 \psi}{\partial r^2} + \frac{\partial^2 \psi}{\partial z^2} = 0 \tag{11}$$

so the flow nets of equipotential surfaces and streamlines are orthogonal, and the function $\psi(r, z)$ is solution of an equation similar to that which describes an even flow; streamlines can be determined by inverse electrical analogy, either with an even resisting network or with conducting paper.

Hence the macroscopic definition of chromatographic flow requires two steps: an outline of equipotential surfaces (Fig. 4) and an outline of streamlines (Fig. 5).

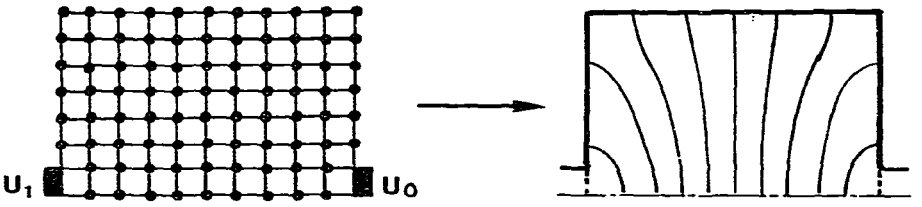

Fig. 4. Direct analogy: outline of equipotential curves.

Determination of λ

In laminar flow, if D_m is sufficiently small or ud_p sufficiently large, the band spreading given by eqn. 4 tends to a limiting value only due to velocity inequalities, *i.e.*, to column-wide flow differences between the axis and column wall; then the end-effect variance, $\sigma^2_{e.c.}$, is determined by the flow profile and column diameter:

$$\sigma^2_{e.c.} = 2\lambda d_c^2 \tag{12}$$

In order to determine $\sigma^2_{e.c.}$, the variance increment undergone by an injection profile of a perfectly rectangular plug shape (sample concentration C_I) and due to the uneven flow pattern in the column extremities must be calculated. For this calculation, diffusion or convective mixing processes are assumed not to occur.

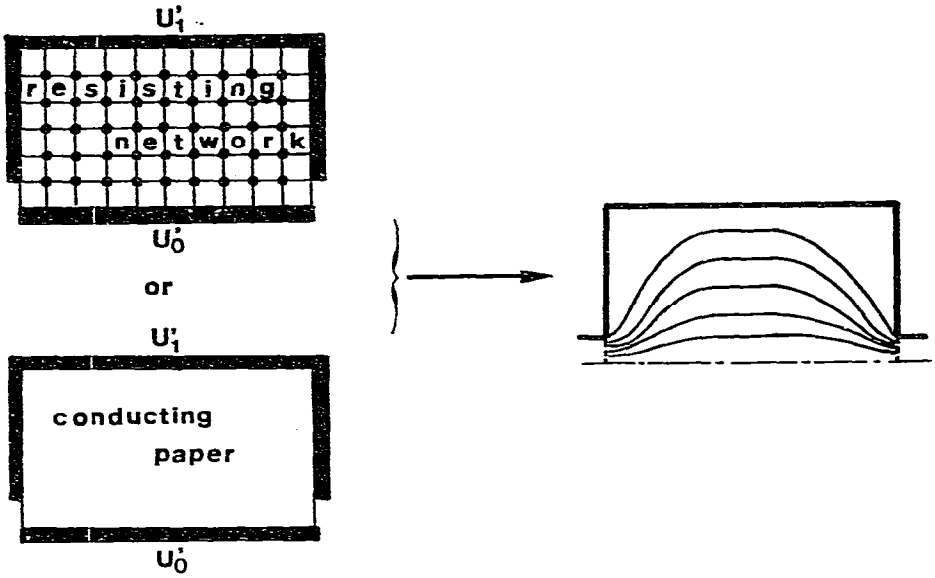

Fig. 5. Inverse analogy: outline of streamlines.

The use of an analogue method allows the determination of the flow net of equipotential curves and streamlines for any end-column geometry (Fig. 1). The velocity at each column point could be calculated from this flow net: $\vec{u} = -k \overrightarrow{\text{grad}}\ \varnothing$, where k is a constant that depends on the porous medium permeability and on the physico-chemical properties of the moving fluid; when l_{ij} is the length on streamline j and between equipotential curves $\varnothing_i$ and $\varnothing_{i+1}$ (Fig. 6) the modulus of the mean velocity vector is given by:

$$|u_{ij}| = \left| -k \cdot \frac{\varnothing_{i+1} - \varnothing_i}{l_{ij}} \right| \tag{13}$$

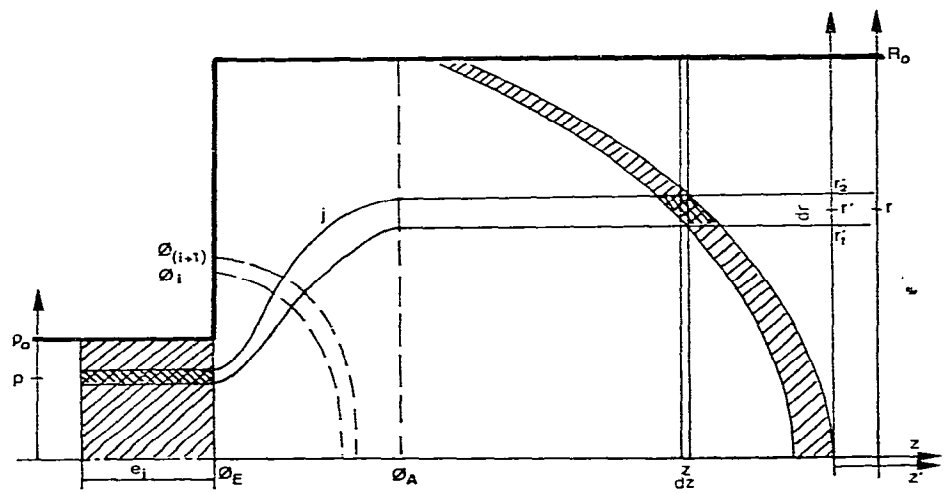

Fig. 6. Schematic representation of the deformation undergone by the eluted band due to end-effects between $\varnothing_0$ and $\varnothing_A$.

Beyond the equipotential curve $\varnothing_A$ the flow field becomes even and there is no longer any velocity inequality on the column cross-section at $\varnothing_A$. The travel time spent in going from the equipotential curve $\varnothing_E$ to the equipotential curve $\varnothing_A$ depends on the channel followed by the liquid flow; this travel time, t_j, is the sum of the elementary ones in the same streamline and between two adjacent equipotential curves:

$$t_j = \sum_{i=0}^{i=n} t_{ij} = \sum_{i=0}^{i=n} \frac{l_{ij}}{|u_{ij}|} \tag{14}$$

From eqns. 13 and 14 we obtain

$$t_j = \sum_{i=0}^{i=n} \left| -\frac{l_{ij}^2}{k(\varnothing_{i+1} - \varnothing_i)} \right| \tag{15}$$

with $\varnothing_0 = \varnothing_E$ and $\varnothing_{n+1} = \varnothing_A$.

Each point of the equipotential curve $\varnothing_A$ is defined by its ordinate r_j; the liquid flux spends a time t_j in reaching this point from $\varnothing_E$. Hence eqn. 15 allows one to draw the plot $r_j = g'(t_j)$, or $r = g'(t)$. Beyond $\varnothing_A$ the eluted band is in an even flow field where the mean velocity is constant and equal to u at each point; hence this band is kept unmodified and its equation is $r = g'(z/u)$ or

$$r = g(z) \tag{16}$$

After introduction of moving coordinates

$$\left.\begin{aligned} z' &= z - ut \\ r' &= r \end{aligned}\right\} \tag{17}$$

Let an elementary channel (Fig. 6) be included between two streamlines that are infinitely near; in laminar flow there is a liquid flux conservation inside the channel, *i.e.*, the solute mass dm introduced at ordinate ϱ of the feed reappears at ordinate r in an elementary channel of thickness dr; under the initial hypothesis the solute concentration in the eluted band is kept constant along the channel. The solute mass, dm, in the elementary channel is given by

$$dm = C_I e_I 2\pi\varrho d\varrho = C_I e_B 2\pi r' dr' \tag{18}$$

where e_I and e_B are the band thickness at the column head and at abscissa z inside the column, respectively; when the flow becomes uniform e_B is constant:

$$e_B = \frac{e_I \beta^2}{\varepsilon_T} \tag{19}$$

where ε_T represents the total porosity of the packed bed. At z' the solute concentration $C_{z'}$ in the elementary volume dV defined by the column cross-section of thickness dz' is equal to dM/dV, with

$$dM = \int_{r_1'}^{r_2'} \frac{d_m d_{z'}}{e_B} = \pi C_I (r_1' + r_2')(r_2' - r_1') \qquad (20)$$

$$dV = \frac{\pi d_c^2 \varepsilon_T d_{z'}}{4}$$

r_1' and r_2' are the ordinates at z' of the tailing and leading fronts of the eluted band. Then C_{z1} is given by

$$C_{z'} = \frac{4C_I}{\varepsilon_T d_c^2}(r_1' + r_2')(r_2' - r_1') \qquad (21)$$

When the injection profile becomes infinitely narrow, e_I and e_B tend to zero and eqn. 21 can be written as

$$C_{z'} = \frac{4C_I e_B 2r'}{\varepsilon_T d_c^2} \cdot \frac{\Delta r'}{e_B} \qquad (22)$$

The limit of $\Delta r'/e_B$ when e_B tends to zero is dr'/dz' ,and eqn. 22 becomes

$$C_{z'} = C_I \cdot \frac{8e_I\beta^2}{\varepsilon_T^2 d_c^2} \cdot r' \cdot \frac{dr'}{dz'} \qquad (23)$$

Then the characteristic peak variance of this band spreading is

$$\sigma_{e.c.}^2 = \frac{\int_0^{z_L'} z'^2 C_{z'}\, dz'}{\int_0^{z_L'} C_{z'}\, dz'} - \left(\frac{\int_0^{z_L'} z' C_{z'}\, dz'}{\int_0^{z_L'} C_{z'}\, dz'} \right)^2 \qquad (24)$$

where z_L' is the total length of the eluted band profile; in order to standardize, we write $r' = yd_c$ and $z' = xd_c$, in which y varies from 0 to 0.5 and x depends only on the general shape of the flow profile in the column extremities: eqns. 12, 23 and 24 allow one to write

$$\lambda = \frac{1}{2}\left[\frac{\int_0^{x_L} x^2 y \cdot \frac{dy}{dx} \cdot dx}{\int_0^{x_L} y \cdot \frac{dy}{dx} \cdot dx} - \left(\frac{\int_0^{x_L} xy \cdot \frac{dy}{dx} \cdot dx}{\int_0^{x_L} y \cdot \frac{dy}{dx} \cdot dx} \right)^2 \right] \qquad (25)$$

EXPERIMENTAL

The determination of the flow field by analogue simulation was performed with a miniaturized resisting network of removable resistances designed by Kastner[16]. Each printed board can receive an even network of 10 × 10 nodes. The network was fed with a direct current by an FMW (Orsay, France) Lambda stabilized power supplier. Voltage and intensity were measured with a Hewlett-Packard (Orsay, France) 3465A

numerical voltmeter. Between two nodes the potential was defined by interpolation; all the data allow one to draw equipotential curves by direct analogy and streamlines by inverse analogy. From the flow net of streamlines and equipotential curves the equation $r' = g(z')$ was adjusted with the following polynomial function by the least-squares method:

$$r' = \sum_{j=2}^{j=n} a_j z'^{1/j} \tag{26}$$

The chromatograph used was assembled from the following elements: TM 380 reciprocating pump (Touzart et Matignon, Vitry/Seine, France), Waters M 6000A reciprocating pump (Waters Assoc., Paris, France), pressure transducer, Rheodyne Model 7105 sample injector (Touzart et Matignon), LDC 1205 UV detector operated at 254 nm (Sopares, Gentilly, France) and Linseis Model LS 24 recorder (Linseis, Selb, G.F.R.).

Home-made columns were used with stainless-steel tubing of dimensions 45 × 4.7 mm I.D., 50 × 7.4 mm I.D. and 60 × 10.7 mm I.D. All columns were packed by a previously described slurry method[17] with irregularly shaped Partisil 20 (d_p = 21 μm) and Partisil 5 (d_p = 5.7 μm) silica gel from Whatman (Ferrieres, France).

In all experiments the eluent was *n*-heptane–ethyl acetate (80:20). The solvents were of high purity and supplied by S.D.S. (Peypin, France) and Rhône-Alpes Chimie (Caluire, France). The sample solutes were chemicals of the highest purity from various suppliers, and were dissolved in the mobile phase.

The injected volume varied from 1 to 5 μl and the sample size was kept sufficiently small to prevent any overloading of the column. The dead volume of each column was determined by injection of carbon tetrachloride; the retention volumes were accurately measured by means of the first statistical moment of the peak and by means of the flow-rate, which was determined volumetrically.

The chromatographic data were stored on floppy discs using a Model MCS Z80 microcomputer (A2M, Paris, France); the Datel MDAS-8D analogue–digital converter (A2M) of the computer was connected to the detector via a home-built amplifier high-frequency filter unit. The data acquisition frequency was programmed in Assembly language. The variance of the chromatographic peaks was calculated by means of the second central moment of the peaks.

All numerical calculations were carried out by computer using BASIC language.

RESULTS AND DISCUSSION

First it is necessary to stress a major point: with our working hypothesis the flow field is identical in both column extremities, the other parameters being kept constant, so the spreading process and the variance determination are identical and the results obtained are applicable at both column ends.

Influence of section ratio β

It has been seen previously (eqn. 12) that band spreading tends to a maximum; this maximum depends on the column diameter and on a parameter λ, which is

proportional only to the flow field shape; λ is equal to $\sigma^2_{e.c.}/2\,d_c^2$ and is calculated from analogue simulation on a resisting network for various β values. Fig. 7 shows the λ *versus* β curve, which is well fitted by the equation

$$\lambda = 0.045\,(1 - \beta)^2 \tag{27}$$

The dependence of λ on β is logical as $\sigma^2_{e.c.}$ is zero if β is unity, *i.e.*, the column is fed on the overall cross-section; in this instance, the flow field is even and end-effects do not exist. λ varies from 0 to $5 \cdot 10^{-2}$; a comparison of these values with those obtained by Giddings[2], Horváth and Lin[5] and Huber[4] for convective mixing in the mobile phase shows a large difference; the values obtained by these workers vary between 5 and 10; however, these last values characterize velocity inequalities at the particle diameter level, but λ calculated in this work is a measure of velocity inequalities at the column diameter level. The ratio between column diameter and particle diameter varies from 100 to 1000 in most common columns and therefore spreading resulting from velocity inequalities by end-effects is several hundred times higher than spreading due to velocity inequalities by convective dispersion in a packed bed.

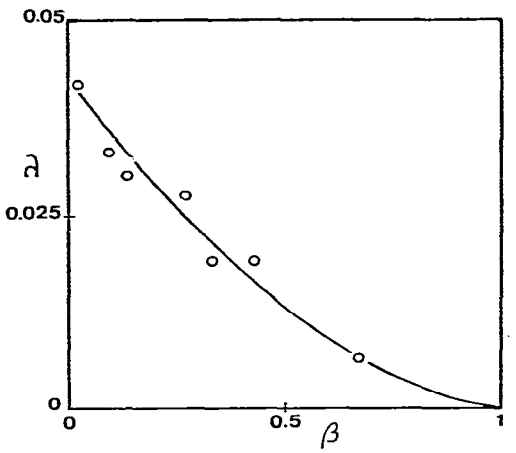

Fig. 7. Graph of velocity inequality parameter λ *versus* section change ratio β.

Influence of porous frits

The chromatographic column is a whole entity and the analyst is interested only in the overall band spreading of this column; one part of this broadening results from the sample dispersion due to the packing bed and another part results from additional effects, such as wall effects, end-effects and the presence at the column extremities of porous frits which are used to maintain the stationary phase particles inside the column. In fact, the presence of these frits modifies the uneven flow field shape and this modification involves an additional dispersive effect on the sample band.

By the analogue simulation method, it is possible to determine the liquid flow through two juxtaposed porous media of different permeabilities, provided that each

of them is homogeneous and isotropic. Let K be the permeability ratio between these two media; resistance values for the whole resisting network are given by eqns. 9 and 10; the ratio between the network constants R is equal to K; in laminar flow, streamlines follow a refraction law when they pass through the interface between two different porous media; a sharp change in the direction of the velocity vector occurs if this vector does not arrive perpendicular to the interface. Therefore, the presence of porous frits modifies the flow field shape and this modification depends on two characteristics of the frits, *viz.* their thickness and their permeability. In order to standardize the results we consider only the permeability of the porous frit relative to that of the packed bed, K_f/K_0, and the thickness of the porous frit relative to the column diameter, e/d_c.

Fig. 8 shows various flow field shapes obtained with the same end-column geometry ($\beta = 0.068$) and different porous frits. In Fig. 8a the flow profile shown is obtained when there is no porous frit; if the porous frit is very thick or its permeability is the same as that of the column, the flow field is identical. The disturbed area extends inside the column up to a distance of about one column radius. In the "dead-corner" lying near the end and wall of the column the pressure drop gradient is low for a longer path; this fact explains the large delay to solute molecules travelling inside these channels. Fig. 8a, b and c show the modifications to the flow pattern when the permeability of the porous frit which was identical with that of the packing becomes 5 or 50 times greater, the frit thickness being kept constant; the uneven flow area becomes more restricted and is finally confined inside the porous frit; then it is

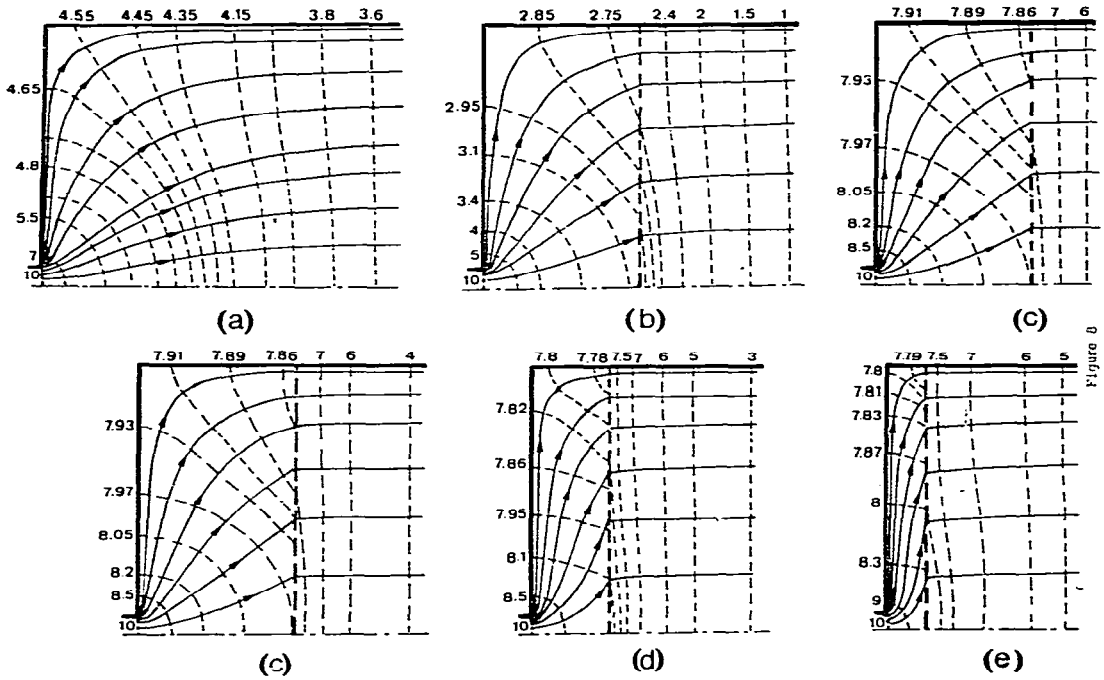

Figure 8

Fig. 8. Flow net of equipotential curves and streamlines for the same column-top geometry ($\beta = 0.068$) and for various frits. (a) No frit; (b) $e/d_c = 0.27$, $K_f = 5\ K_0$; (c) $e/d_c = 0.27$, $K_f = 50\ K_0$; (d) $e/d_c = 0.135$, $K_f = 50\ K_0$; (e) $e/d_c = 0.07$, $K_f = 50\ K_0$.

no longer possible to obtain a decrease in band spreading by means of increasing the permeability of the porous frit. Fig. 8c, d and e show the modifications to the flow profile when the permeability of the porous frit is kept constant and its thickness varies. In this instance the evolution is clear: when the thickness of the porous frit decreases the flow field becomes even. Fig. 8 illustrates the important point that for all flow profiles, velocity inequalities between the "dead-corners" and the axis of the column are nearly identical, but the differences result from the distance between the two velocity extremes, and this last parameter determines the magnitude of band spreading.

If β is kept constant for the same end-column geometry and the band spreadings for end-effects with and without a porous frit are called $\sigma^2_{e.c.f.}$ and $\sigma^2_{e.c.}$, respectively, the influence of the relative porous frit permeability (Fig. 9) and the relative porous frit thickness (Fig. 10) is expressed by the ratio $\sigma^2_{e.c.f.}/\sigma^2_{e.c.}$.

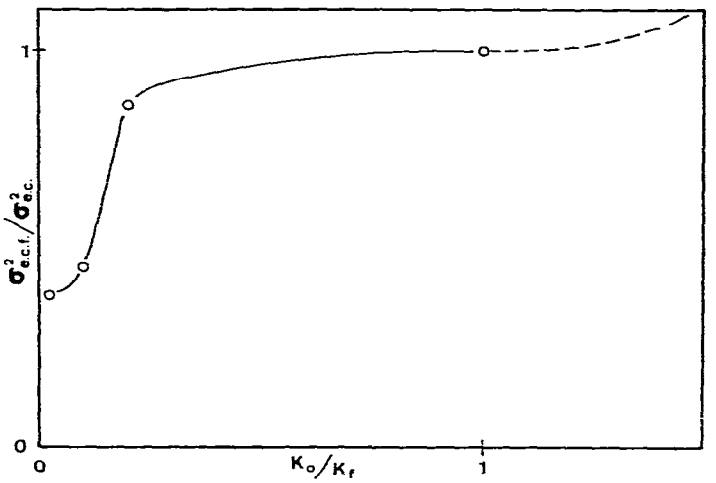

Fig. 9. Graph illustrating the effect of frit permeability on band spreading due to end-effects.

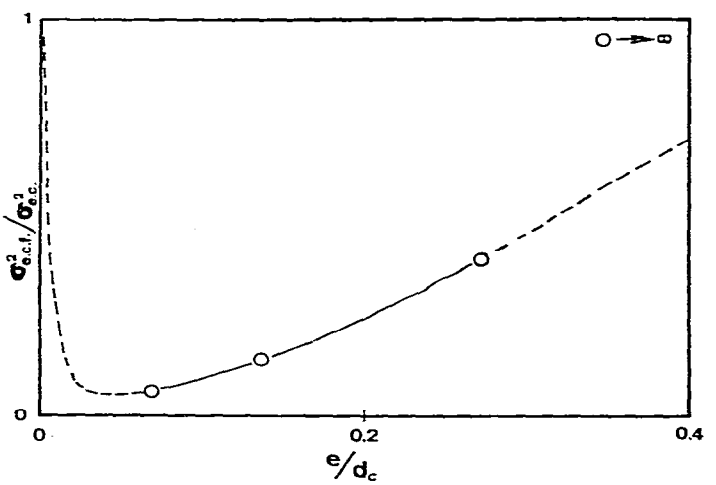

Fig. 10. Graph illustrating the effect of frit thickness on band spreading due to end-effects.

These last two figures indicate the importance of frits; when the permeability of the frit increases relative to that of the packing, the peak variance either reaches a minimum or tends to a limiting value (which seems more probable); nevertheless, it is impossible by analogue simulation to verify this last point because it is nearly impossible to simulate in practice such a large permeability inequality on a resisting network. In the same way, when the thickness of the frit decreases, the peak variance reaches a minimum equal to 10% of the initial value (without the frit); it seems that this optimal value should be obtained for a frit thickness less than 0.05 d_c. Figs. 9 and 10 seem to demonstrate that, for a given column diameter and packing permeability, there is an optimal choice for the thickness and the permeability of the porous frit. Now, it is difficult to state precisely rules that determine these optimal conditions; however, we think that a sufficiently correct approximation is obtained by choosing the porous frit on the basis of the criteria $K_f \approx 50\ K_0$ and $e \approx 0.05\ d_c$. Some mistakes must be strictly avoided: using porous frits with a permeability equal to or less than that of the packing and choosing frit thicknesses of the same order of magnitude as the column diameter; obviously this advice is relevant only if the end-effects are noticeable.

Coupling and end-effects

A study of peak broadening involves the contribution of independent factors of which the second moments, or peak variances (σ^2), are additive according to the relationship

$$\sigma_T^2 = \sigma_{\text{col.}}^2 + 2\sigma_{\text{e.c.}}^2 + \sigma_{\text{e.e.}}^2 \tag{28}$$

where σ_T^2 is the total observed variance with end-effects, $\sigma_{\text{col.}}^2$ is the column variance without end-effects and $\sigma_{\text{e.e.}}^2$ represents the sum of the variances due to injection system, connectors and detectors (the so-called external effects).

In order to determine $\sigma_{\text{e.c.}}^2$ we proceed as follows:

(1) Without the column, peak broadening is determined with and without a sampling valve.

(2) Secondly, the peak variance, $\sigma_{\text{col.}}^2$, is measured with the following injection mode: the sample is introduced into the column at the centre of the cross-section on to the inlet frit while the flow of mobile phase is directed across the entire column inlet cross-section. This mode of sample introduction produces a sharp sample pulse into the centre of the column, and the integrity of this plug is maintained while it passes through the centre of the column bed; injection is accomplished by means of a syringe.

(3) Finally, the peak variance, σ_T^2, is determined for the same column and with identical end-effects at each column extremity, by using an identical zero dead-volume fitting to close both extremities of the column and connecting the column head with a sampling valve.

Under these conditions $\sigma_{\text{e.c.}}^2$ is given by

$$\sigma_{\text{e.c.}}^2 = \tfrac{1}{2}(\sigma_T^2 - \sigma_{\text{col.}}^2 - \Delta\sigma_{\text{e.e.}}^2) \tag{29}$$

$\Delta\sigma_{\text{e.e.}}^2$ represents the difference in the peak variances, originating in the external part, included between sample valve injection and injection by syringe.

As an example with one column, Fig. 11 demonstrates the graphs of σ_T^2, $\sigma_{col.}^2$ and $\Delta\sigma_{c.c.}^2$ *versus* flow-rate of mobile phase; within the range of flow-rates investigated $\Delta\sigma_{c.c.}^2$ represents about half of the overall extra-column effects.

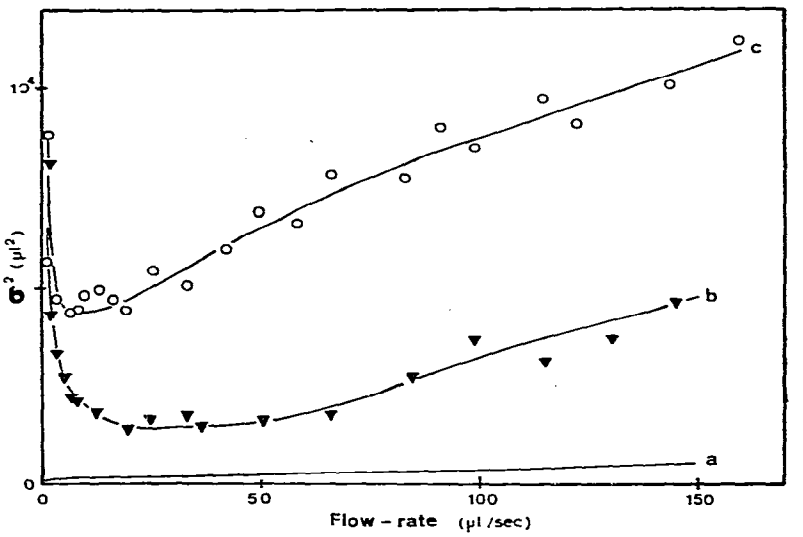

Fig. 11. Plots of variance *versus* flow rate for 9-methylanthracene ($k' = 0.21$). Column, 5 cm × 7.4 mm I.D.; frit, $e = 2$ mm, $K_f = 8\,K_0$; stationary phase, Partisil 5; mobile phase, *n*-heptane–ethyl acetate. (a) $\Delta\sigma_{c.c.}^2$; (b) variance without end-effects; (c) peak variance with end-effects.

It is not our purpose to generalize the discussion about this last example, but some observations can be made. Firstly, even with such a short column, the contribution of the sampling valve to peak broadening is relatively low, being about 5% of σ_T^2, but at the same time the variances $\Delta\sigma_{c.c.}^2$ and $\sigma_{c.c.}^2$ represent 17% and 34%, respectively, of $\sigma_{col.}^2$. Secondly, even in this instance, which is not extreme, end-effects are responsible for a very large increase in the peak variance. Finally, without end-effects the efficiency of the column is good because the minimum of the variance $\sigma_{col.}^2$ corresponds to a theoretical plate height of 17 μm, and if extra-column effects are substracted the plate height of the column reaches 12 μm or about 2.1 d_p.

Fig. 12 shows the graph of $\sigma_{c.c.}^2$ *versus* linear velocity of the mobile phase for various column diameters and various β ratios. In this instance the porous frit and packing had the same permeability and the determination of $\sigma_{c.c.}^2$ without a porous frit is possible. These plots are characteristic of a coupling process in the mobile phase according to eqn. 4; at very low velocity, the residence time in the extremities is sufficiently large to involve considerable mass transfer between the low-velocity and the high-velocity channels; the variance decreases and tends to zero. However, this decrease in band spreading is noticeable only at velocities lower than 0.5 mm/sec, and such velocities are not of great interest. In contrast, for the most commonly used velocities in HPLC, the variance $\sigma_{c.c.}^2$ tends rapidly to an asymptotic value that characterizes peak broadening due only to column-wide flow differences and, as shown in Table I, these limiting values are of the same order of magnitude as the variances

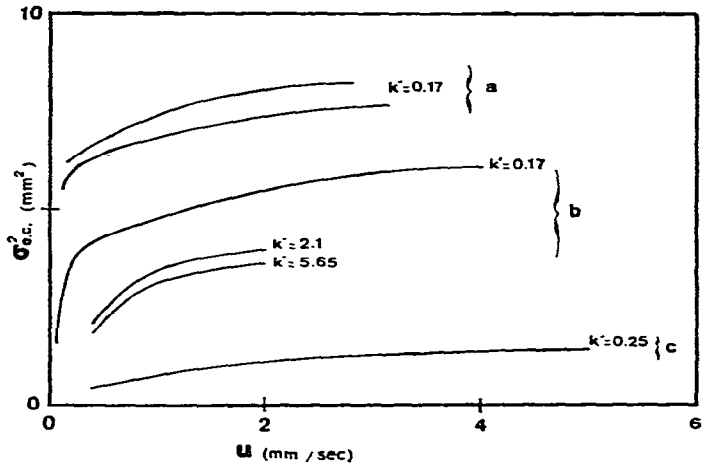

Fig. 12. Plots of variance *versus* velocity. (a) $d_c = 10.7$ mm, $\beta = 0.047$; (b) $d_c = 7.4$ mm, $\beta = 0.068$; (c) $d_c = 4.6$ mm, $\beta = 0.109$. Stationary phase, Partisil 20; mobile phase, *n*-heptane–ethyl acetate; solutes, 9-methylanthracene ($k' = 0.2$), *p*-methoxyacetophenone ($k' = 2.1$) and linuron ($k' = 5.65$).

TABLE I

COMPARISON BETWEEN THE LIMITING VALUES OF THE VARIANCES $\sigma^2_{e.c.}$ OBTAINED BY CHROMATOGRAPHIC MEASUREMENT (FIG. 12) AND THOSE DETERMINED FROM THE FLOW FIELD PROFILE (EQNS. 12 AND 27)

d_c (mm)	β	$\sigma^2_{e.c.}$ (mm²)	
		From Fig. 12	*From eqns. 12 and 27*
10.7	0.047	8.4*	9.0
7.4	0.068	5.1**	4.1
4.6	0.109	1.6	1.5

* Average on two columns.
** Average on three solutes.

$\sigma^2_{e.c.}$ calculated from the flow field profile. Experimental results are in good agreement with the theoretical predictions deduced from the flow profile analysis.

When the permeabilities of the packing and porous frit are different, the flow field profile and the variance are modified. Fig. 13 shows the influence of the permeability of the porous frit on the variance $\sigma^2_{e.c.}$ (the thickness of the frit is kept constant).

It appears from Fig. 13 that the limiting values of the variance change very little when the permeability of the frit becomes 10 times higher than that of the packing; this is in agreement with the results in Fig. 9, where the most important change in the variance occurs when the permeability of the frit becomes 4–8 times higher than that of the packing. The shape of the plots in Fig. 13 is similar to those in Fig. 12 and is also characteristic of a coupling process in the mobile phase; we shall later propose an interpretation for the unexpected decrease in variance (curve b). When the permeability of the porous frit is 10 or more times higher than that of the packing, the presence of the frits is very beneficial because the variance is divided by a factor of 2.

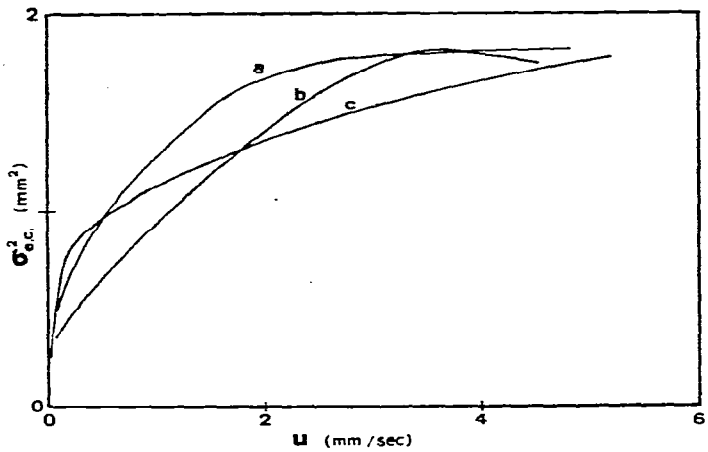

Fig. 13. Plots of variance *versus* velocity for various permeabilities of the frit. (a) $K_f = 8\,K_0$; (b) $K_f = 50\,K_0$ (c); $K_f = 75\,K_0$. $d_c = 7.4$ mm; $\beta = 0.068$; $e = 2$ mm; stationary phase, Partisil 5; mobile phase, *n*-heptane–ethyl acetate; solute, 9-methylanthracene ($k' = 0.2$).

Fig. 14 shows the graph of variance *versus* mobile phase velocity for various thicknesses and a constant permeability of the porous frit. The plots are similar to those in the preceding figures for low velocities because the spreading process in this flow-rate range is the same and has been largely explained in the preceding comments. When the mobile phase velocity, u, increases, at first the variance also increases, for reasons already given; however, it subsequently reaches a maximum and finally tends to a minimum; this last part of the curves cannot be explained only by the theory given at the beginning of this work, because according to this theory the variance $\sigma^2_{e.c.}$ is a continuously increasing function of u. In our model the molecular diffusion process is taken into account only for the transport of solute molecules from velocity extremes

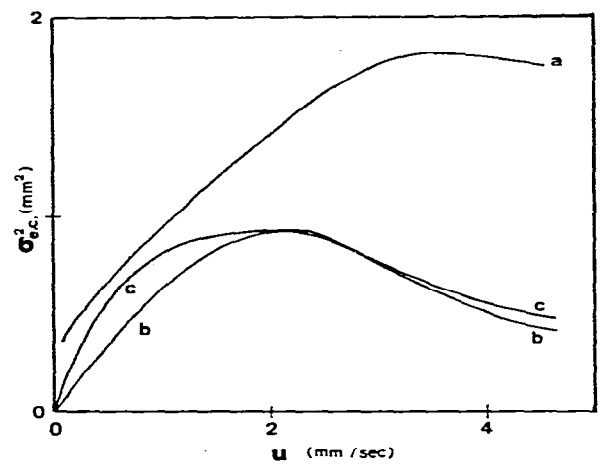

Fig. 14. Plots of variance *versus* velocity for various thicknesses of the frit. (a) $e = 2$ mm; (b) $e = 1$ mm; (c) $e = 0.5$ mm. $d_c = 7.4$ mm; $\beta = 0.068$; $K_f = 50\,K_0$; stationary phase, Partisil 5; mobile phase, *n*-heptane–ethyl acetate; solute, 9-methylanthracene ($k' = 0.2$).

in trans-column effects; however, as was first shown by Van Deemter *et al.*[1] and later by Giddings[2] in a more sophisticated fashion, mass transfer phenomena can also occur by a flow mechanism; Van Deemter *et al.*[1] stated that mass transfer by flow does not depend on fluid velocity, whereas Giddings proposed that this transport depends on the mobile phase velocity, and increases with it, as has been shown by other studies of flow in porous media (Sheidegger[13], p. 306) where the coefficient of lateral dispersion in the moving fluid is constant at low flow-rates and varies linearly with u at high flow-rates. Hence, when the frit has a small thickness and is much more permeable than the packing, the liquid flux inside the frit is roughly perpendicular to the column axis, and when the mobile phase velocity, u, has a value of 4 or 5 mm/sec inside the packing, it reaches several tens of cm/sec at some points inside the frit, as shown in Fig. 8b, d and e. Under these conditions, the flow mechanism plays a substantial role; the thickness of the frit and the difference between the velocity extremes also decrease, indicating that mass transfer between velocity extremes is important and tends to reduce band spreading resulting from velocity inequalities.

From Figs. 13 and 14 it can be deduced that porous frits have a considerable influence on peak broadening because, for this example of column, the use of a frit with a thickness of 0.5 mm and 50 times more permeable than the packing, the variance $\sigma^2_{e.c.}$ is reduced by a factor of 5 and the HETP decreases from 200 to about 40 μm. In order to introduce the influence of porous frits on $\sigma^2_{e.c.}$, eqns. 4 and 27 allow one to write

$$\sigma^2_{e.c.} = \frac{0.09\, d_c^2(1-\beta)^2\, F}{1 + \omega\left(\frac{D_m}{u d_p}\right)^n} \tag{30}$$

F is proportional to e/d_c and K_0/K_f.

Because it is impossible to increase indefinitely the permeability of the frit, there is in any event an optimal value of the thickness, e, for which the variance $\sigma^2_{e.c.}$ is minimal. The maximal permeability of the porous frit seems to be about 50 K_0 and the optimal thickness is 0.1 d_c; under these conditions the initial variance is reduced by a factor of 5; this is summarized by the following relationships:

$$(K_f)_{opt.} \approx 50\, K_0 \tag{31}$$

$$e_{opt.} \approx 0.1\, d_c \tag{32}$$

$$(\sigma^2_{e.c.})_{min.} \approx \frac{0.02\, d_c^2(1-\beta)^2}{1 + \omega\left(\frac{D_m}{u d_p}\right)^n} \tag{33}$$

CONCLUSIONS

The analogue simulation with a resisting network seems to be an excellent method for determining the laminar flow field in chromatographic columns with a homogeneous and isotropic packing; the flow profile analysis makes possible the calculation of the maximal peak variance due to end-effects; in most instances the

results of experimental chromatographic measurements are in good agreement with theoretical predictions.

So far only the results obtained by Kirkland *et al.*[9] can be compared with our spreading model: for a 15 cm × 7.8 mm I.D. column Kirkland *et al.* obtained, for a totally excluded and unretained compound, 8485 plates with syringe injection (without end-effects) and 980 plates with "normal" valve injection (with end-effects); these two results were determined by means of the moment analysis at a mobile phase velocity of 7.3 mm/sec. From these data, eqn. 29 allows $\sigma^2_{e.c.}$ to be calculated as 10 mm², which is of the same order of magnitude as the predicted value from our model (5 mm²). The difference can be explained by the presence of frits with a lower permeability than that of the column.

This work shows that end-effects, even under the best conditions, have a noticeable influence on the overall column efficiency, especially for short columns or largediameter columns. By choosing the optimal characteristics of the porous frits with eqns. 31 and 32, the contribution

$$(H_{e.c.})_{min.} = 2\,(\sigma^2_{e.c.})_{min.}/L \tag{34}$$

to the total column HETP is as shown in Table II for various column conditions and when $\omega(D_m/ud_p)^n \ll 1$, which is often the case in modern liquid chromatography.

TABLE II

PLATE HEIGHTS ($H_{e.c.}$, μm) RESULTING FROM END-EFFECTS (EQN. 34) FOR VARIOUS COLUMN LENGTHS AND VARIOUS DIAMETERS OF THE COLUMN, d_c, AND CONNECTING TUBE, d_a

Column length (cm)	d_c *(mm)*				
	*3**	*4.6**	*7.4**	*10.7***	*20***
5	5.0	14	38	75	290
10	2.5	6.7	19	38	140
15	1.6	4.4	13	25	96
20	1.25	3.4	9.5	19	72
30	0.8	2.2	6.5	13	48
50		1.3	3.8	7.5	29
100		0.7	1.9	3.7	14

* $d_a = 0.5$ mm.
** $d_a = 1.0$ mm.

The following conclusions can be suggested:

(i) in order to eliminate totally the phenomena at column extremities by using a sampling valve it is necessary to introduce the sample by a split-stream injection technique as in analytical chromatography[9,10,18,19] or preparative chromatography[11,20–22];

(ii) in order to reduce to a minimum the variance resulting from end-effects, without the use of a particular injection mode, the characteristics of the frits must be chosen with regard to eqns. 31 and 32;

(iii) in analytical chromatography, the use of very short columns (≤ 5 cm) removes the need for a sampling valve; syringe injection or the use of an injection valve with a split-stream technique is necessary;

(iv) in preparative chromatography, the use of particles of small size involves the development of particular injection devices in order to minimize end-effects.

REFERENCES

1 J. J. Van Deemter, F. J. Zuiderweg and A. Klinkenberg, *Chem. Eng. Sci.*, 5 (1956) 271.
2 J. C. Giddings, *Dynamics of Chromatography*, Marcel Dekker, New York, 1965, p. 52.
3 J. H. Knox, *Anal. Chem.*, 38 (1966) 1255.
4 J. F. K. Huber, *J. Chromatogr. Sci.*, 7 (1969) 85.
5 Cs. Horváth and H.-J. Lin, *J. Chromatogr.*, 126 (1976) 401.
6 J. H. Knox and J. F. Parcher, *Anal. Chem.*, 41 (1969) 1599.
7 J. C. Giddings, *J. Chromatogr.*, 16 (1964) 444.
8 Cs. Horváth and H.-J. Lin, *J. Chromatogr.*, 149 (1978) 43.
9 J. J. Kirkland, W. W. Yau, H. J. Stoklosa and C. H. Dilks, *J. Chromatogr. Sci.*, 15 (1977) 303.
10 B. Coq, G. Cretier and J. L. Rocca, *Chromatographia*, 11 (1978) 461.
11 A. W. J. De Jong, H. Poppe and J. C. Kraak, *J. Chromatogr.*, 148 (1978) 127.
12 L. K. Smith, M. M. Myers and J. C. Giddings, *Anal. Chem.*, 49 (1977) 1750.
13 A. E. Sheidegger, *The Physics of Flow Through Porous Media*, University of Toronto Press, Toronto, 3rd ed., 1974.
14 P. Huard de la Marre, *Publ. Sci. Tech. Minist. Air (Fr.)*, 340 (1958).
15 G. Liebmann, *Brit. J. Appl. Phys.*, 5 (1954) 362.
16 R. Kastner, *Thesis*, Lyon, 1974.
17 B. Coq, C. Gonnet and J.-L. Rocca, *J. Chromatogr.*, 106 (1975) 249.
18 T. J. N. Webber and E. H. McKerrell, *J. Chromatogr.*, 122 (1976) 243.
19 H. Colin, J. C. Diez-Masa, M. Martin, A. Jaulmes and G. Guiochon, *J. Chromatogr.*, to be published.
20 B. Coq, G. Cretier and J. L. Rocca, *J. Chromatogr.*, in press.
21 E. Godbille and P. Devaux, *J. Chromatogr.*, 122 (1976) 317.
22 G. Ferraris and M. Lauret, *Anatusis*, in press.